

Ferroelectric ordering and magnetoelectric effect of pristine and Ho-doped orthorhombic DyMnO₃ by dielectric studies

J. Magesh, P. Murugavel¹, R. V. K. Mangalam, K. Singh, Ch. Simon, and W. Prellier

Citation: *J. Appl. Phys.* **118**, 074102 (2015); doi: 10.1063/1.4928965

View online: <http://dx.doi.org/10.1063/1.4928965>

View Table of Contents: <http://aip.scitation.org/toc/jap/118/7>

Published by the [American Institute of Physics](#)

Ferroelectric ordering and magnetoelectric effect of pristine and Ho-doped orthorhombic DyMnO₃ by dielectric studies

J. Magesh,¹ P. Murugavel,^{1,a)} R. V. K. Mangalam,² K. Singh,² Ch. Simon,² and W. Prellier²

¹Department of Physics, Indian Institute of Technology Madras, Chennai 600036, India

²Laboratoire CRISMAT, ENSICAEN/CNRS UMR 6508, 6 Bd Maréchal Juin, 14050 Caen, France

(Received 5 June 2015; accepted 9 August 2015; published online 20 August 2015)

In this paper, the magnetoelectric coupling and ferroelectric ordering of the orthorhombic Dy_{1-x}Ho_xMnO₃ ($x = 0$ and 0.1) are studied from the magnetodielectric response of the polycrystalline samples. The dielectric study on the DyMnO₃ reveals ferroelectric transition at 18 K along with an addition transition at 12 K. We suggest that the transition at 12 K could have originated from the polarization flop rather than being the rare earth magnetic ordering. The magnetodielectric study reveals a magnetoelectric coupling strength of 10%, which is stronger by two orders of magnitude in comparison to the hexagonal manganites. Surprisingly, the Ho³⁺ substitution in DyMnO₃ suppresses the magnetoelectric coupling strength via the suppression of the spiral magnetic ordering. In addition, it also reduces the antiferromagnetic ordering and ferroelectric ordering temperatures. Overall, the studies show that the rare earth plays an important role in the magnetoelectric coupling strength through the modulation of spiral magnetic structure. © 2015 AIP Publishing LLC.

[<http://dx.doi.org/10.1063/1.4928965>]

I. INTRODUCTION

Multiferroics having several ferroic orders received lot of attention due their wide variety of technological applications.^{1,2} The inherent magnetoelectric coupling gives an additional degree of freedom in device fabrication. Although, the existence of multiferroic materials is predicted few decades early,^{3,4} the recent revival of this field is due to the observation of multiferroicity in new class of materials.⁵⁻⁹ Among them, the RMnO₃, where R is a rare earth element, is interesting due to its low dielectric loss. RMnO₃ crystallizes in orthorhombic phase for larger ionic radii R^{3+} (La to Dy), whereas it crystallizes in hexagonal phase for smaller ionic radii R^{3+} (Ho-Lu, Y and Sc) at ambient temperature and pressure.¹⁰ The RMnO₃ with smaller/larger R^{3+} ionic radii can also be crystallized in orthorhombic/hexagonal phase by high pressure synthesis and by highly strained epitaxial film fabrication methods.¹¹⁻¹⁴ The magnetic structure of the orthorhombic RMnO₃ varies from A-type antiferromagnetism for larger R^{3+} ionic radii ($R^{3+} = \text{La to Pr}$) to E-type antiferromagnetism for smaller R^{3+} ionic radii ($R^{3+} = \text{Ho to Lu}$). Interestingly, the structure exhibits modulated spiral magnetic structure for intermediate R^{3+} ionic radii ($R^{3+} = \text{Gd, Tb, and Dy}$).^{15,16} The spiral magnetic ordering is suggested to drive the onset of ferroelectricity in these manganites, though the ferroelectricity is claimed in E-type manganites as well.¹⁶⁻¹⁹ However, the polarisation value ($0.1 \mu\text{C}/\text{cm}^2$) is two-orders weaker in magnitude in comparison to the conventional ferroelectrics.¹⁷ Such low-polarisation magnitude generally arises from the improper ferroelectrics, where the symmetry requirements are not strictly maintained.

Interestingly the orthorhombic DyMnO₃, located at the phase boundary, is expected to show strong magnetoelectric

coupling. The DyMnO₃ is reported to exhibit the transitions at 40, 18, and 6 K.^{16,20,21} The transition at 6 K is due the rare earth ordering (T_N^{Dy}) and the one at 40 K is attributed to Mn³⁺ collinear incommensurate antiferromagnetic ordering (T_N^{Mn}).^{16,20} But the transition at 18 K is ascribed to the spiral magnetic ordering.²² These magnetic transitions are mostly inferred indirectly from the specific heat and dielectric measurements due to the masking effect of high paramagnetic Dy³⁺ magnetic moment.^{16,23} The spiral magnetic ordering breaks the inversion symmetry and thus sets the onset of ferroelectric ordering (T_C). An additional transition is reported at 12 K whose origin is not clear.^{21,24} Few workers attributed it to the rare earth ordering and few others claimed it as polarization flop transition due to the change in magnetic structure.^{21,24} The concurrence of the magnetic and ferroelectric ordering generally results in strong coupling between the order parameters. However, the role of rare earth in the ferroelectric ordering and magnetoelectric coupling remains largely unexplored. The magnetoelectric coupling in orthorhombic DyMnO₃ is attributed to the presence of Dzyaloshinskii-Moriya interaction, which couples the ferroelectricity and incommensurate magnetism.²⁵ The interaction strength depends on the overlap of neighbouring Mn³⁺ spins via the oxygen. The bond-angle connecting the Mn-O-Mn plays an important role.²⁶ Upon decreasing the ionic radii of rare earth, the octahedral tilt of MnO₆ increases.²³ This leads to strong interaction between the neighbouring spins which in turn expected to enhance the magnetoelectric coupling strength. In this paper, we have substituted DyMnO₃ with smaller ionic radii Ho³⁺ ion and studied their magnetoelectric effect. The Ho³⁺ substitution is expected to increase the octahedral tilt and thereby enhance the magnetoelectric coupling. Surprisingly, though the DyMnO₃ shows two orders of magnitude stronger magnetoelectric effect in comparison to the hexagonal manganites, the rare earth doping suppresses

^{a)}Electronic mail: muruga@iitm.ac.in

the coupling. The effect of rare earth on the ferroelectric transition and the magnetoelectric coupling are presented in this work.

II. EXPERIMENTAL DETAILS

Polycrystalline $\text{Dy}_{1-x}\text{Ho}_x\text{MnO}_3$ ($x = 0$ and $0.1, 0.3, 0.4, 0.5$, and 1) are synthesized by conventional solid state technique. Initially, the parent compounds DyMnO_3 and HoMnO_3 were synthesized from the stoichiometric amount of Dy_2O_3 , Ho_2O_3 , and Mn_2O_3 precursors. The stoichiometric proportions of the parent compounds are then ground well and calcinated at 1350°C for 12 h for several times to get uniform composition. Powder X-ray diffraction (XRD) patterns are obtained for the polycrystalline $\text{Dy}_{1-x}\text{Ho}_x\text{MnO}_3$ using a PANANALYTIC X-ray diffractometer. In order to measure the capacitance at low temperatures, Agilent 4248 RLC bridge is integrated to Physical Property Measurement System (PPMS) to vary the temperature from 10 to 300 K. The magnetodielectric responses are studied at 10 K under various magnetic fields from 0 to 14 T by employing the Quantum Design Physical Properties Measurements System.

III. RESULTS AND DISCUSSION

As the Dy^{3+} and Ho^{3+} lie at the phase boundary of the orthorhombic and hexagonal RMnO_3 , a solid solution gives an idea about the competition between the two ions in determining the structural phase diagram. In order to study the phase stability, XRD patterns of polycrystalline $\text{Dy}_{1-x}\text{Ho}_x\text{MnO}_3$ are obtained and are shown in Fig. 1. Earlier studies on Dy^{3+} substituted HoMnO_3 suggest that the hexagonal phase is highly stable due to its accommodative nature, thus forming a single phase solid solution up to $x = 0.5$.²⁷ On the other hand, the

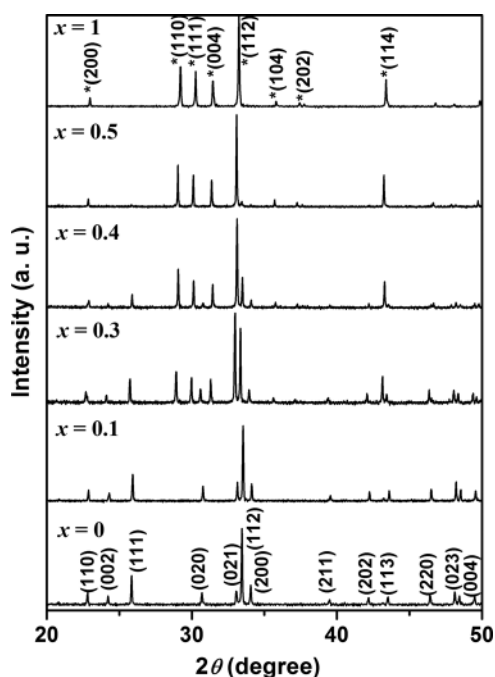


FIG. 1. The XRD patterns of $\text{Dy}_{1-x}\text{Ho}_x\text{MnO}_3$. The peaks corresponding to the hexagonal phase are marked by the symbol *.

orthorhombic phase is relatively unstable while accommodating the smaller Ho^{3+} ion. As a result, the compounds crystallized in orthorhombic phase for $x = 0.1$ show mixed phases for the compositions $x = 0.3, 0.4$, and 0.5 as shown in Figure 1. The lattice parameters a , b , and c of DyMnO_3 are found to be 5.41, 5.71, and 7.14 Å, respectively. Upon increasing the Ho^{3+} concentration to $x = 0.1$, the lattice parameters decrease which is in accordance with the decreased ionic radii of Ho^{3+} . For $x = 0.3$, the competing hexagonal and orthorhombic interactions lead to the formation of mixed phases. The mixed phases are indexed according to the hexagonal and orthorhombic phases. However, the ratio of the intensity of the high intensity (112) peak of the hexagonal phase to that of the orthorhombic phase ($h = 1.18$) indicates the competent nature of these phases in $\text{Dy}_{0.7}\text{Ho}_{0.3}\text{MnO}_3$. On further increase in Ho^{3+} to $x = 0.4$, the hexagonal phase dominates over the orthorhombic phase ($h = 2.64$). Surprisingly, the 1:1 substitution of Dy^{3+} and Ho^{3+} results in almost hexagonal phase ($h = 10.6$). Though the dielectric and magnetoelectric studies are carried out on all samples, to avoid confusion, the results are presented only on phase pure orthorhombic $\text{Dy}_{1-x}\text{Ho}_x\text{MnO}_3$ ($x = 0$ and 0.1) samples.

The dielectric constant is measured as a function of temperature from 8 to 300 K at frequencies ranging from 5 to 100 kHz for polycrystalline DyMnO_3 and the resultant graphs are shown in Fig. 2(a). The dielectric constant shows a broad dispersive behavior above 170 K. The sharp increase in the dielectric constant around 170 K is attributed to the thermal excitation of the charge carriers responsible for the conductivity of the samples. Earlier reports suggest that

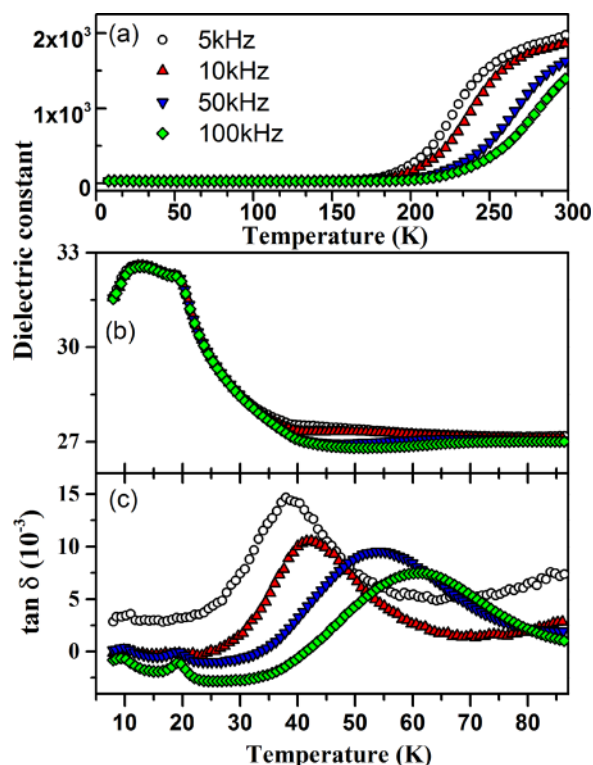


FIG. 2. (a) The dielectric constant of DyMnO_3 plotted at various frequencies from 300 to 8 K. The temperature-dependent (b) dielectric constant and (c) dielectric loss factor at various frequencies plotted at low temperature range.

the nearest neighbour hopping conduction which follows the Arrhenius theory of activation leads to the sharp increase in the dielectric constant.²⁸ Such charge excitation contribution to the polarisation is ascribed as the Maxwell-Wagner mechanism.²⁸ However, below 150 K, the dielectric constant shows subtle changes and the loss-factor is less than 0.1. This indicates the suppression of Maxwell-Wagner contribution and the insulating behavior of the sample. Thus, we believe that the dielectric response below 150 K is intrinsic in origin, i.e., innate dielectric response of the sample.

Figures 2(b) and 2(c) show the evolution of dielectric constant and dielectric loss upon decreasing the temperature from 95 to 8 K. The dielectric constant shows a slope change at 75 K accompanied by the onset of dispersive behavior which is persisting up to 40 K. At 40 K, the dielectric constant increases sharply where the incommensurate collinear ordering of the Mn^{3+} (T_{N}^{Mn}) is said to happen.²⁹ Note that the magnetic measurements do not reveal the Mn^{3+} ordering as it is masked by high paramagnetic moment of Dy^{3+} . The dielectric constant shows another sharp slope change at 18 K which is generally attributed to the onset of spiral ordering induced ferroelectric displacements. Earlier studies indicate that the onset of spiral magnetic ordering along the *b*-axis induces the polarization along the *c*-axis via inverse Dzyaloshinskii-Moriya interaction. Upon further decrease in temperature, up to 12 K, the dielectric constant shows plateau region and then drops down rapidly. Few researchers claimed that the rare earth ordering occurs at temperature as high as 12 K.²¹ On the other hand, it has been attributed to the switching of the spiral magnetic ordering which in turn switches the polarization from *c* to *a*-axis.^{16,24}

The dielectric loss shown in Fig. 2(c) reveals the presence of three peaks. The peaks around 10 K and 18 K show nearly a frequency independent behavior. Whereas the peak around 40 K shows a frequency dispersive behavior. The frequency dependent dielectric loss is an effective tool to differentiate the various contributions to the dielectric constant, such as pure magnetic ordering, magnetic ordering driven ferroelectric transition, and thermal excitations. Pure magnetic ordering will not exhibit a peak in the dielectric loss spectrum, whereas the ferroelectric transition driven by the magnetic ordering could exhibit a peak in the dielectric loss spectrum. In DyMnO_3 , the collinear sinusoidal antiferromagnetic ordering at T_{N}^{Mn} (40 K) being purely magnetic in origin will not be revealed in the dielectric loss spectrum. Hence, the observed broad peak in Fig. 2(c) and its frequency dispersive behaviour suggest that it can be attributed to the variable range hopping (VRH) of the polaronic conduction in the sample.^{22,28} On the other hand, the frequency independent character of the peaks at 18 K and 12 K could originate from the ferroelectric transitions accompanying the magnetic ordering. Hence, the dielectric studies suggest that the transition at 12 K could be assigned to the switching of polarisation (polarization flop transition $T_{\text{PF}}^{\text{Mn}}$) rather than the rare earth magnetic ordering.

To study the effect of magnetic field on the magnetic ordering, the dielectric constant as a function of temperature is measured at various external applied magnetic fields and they are shown in Fig. 3(a). The transition at 40 K did not

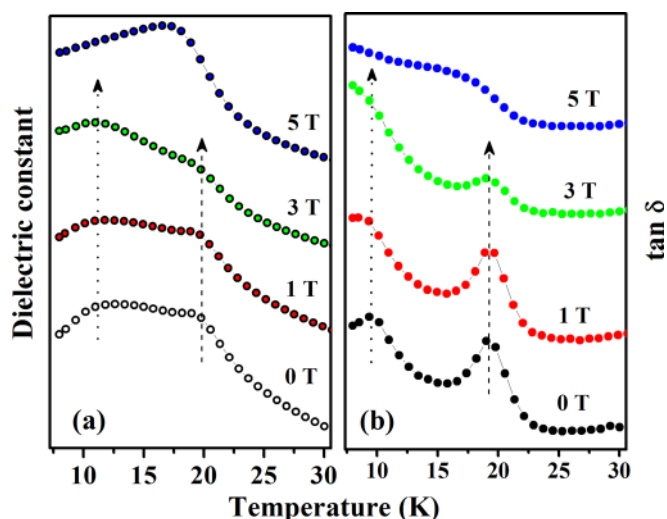


FIG. 3. The temperature-dependent (a) dielectric constant and (b) dielectric loss plotted at various magnetic fields near the ferroelectric ordering temperature.

show any appreciable variation with magnetic field (not shown in the figure). The T_{C} at 18 K and the $T_{\text{PF}}^{\text{Mn}}$ at 12 K remain unperturbed up to 3 T. However, the trends in slope change near these transitions strongly indicate that the applied magnetic field suppresses the ferroelectric ordering and favors a polarization flip from *c* to *a* axis. In agreement with the earlier reports, at 5 T, the T_{C} shifts to a lower temperature and the $T_{\text{PF}}^{\text{Mn}}$ vanishes.³⁰ In Fig. 3(b), the dielectric loss is plotted as a function of temperature near T_{C} and $T_{\text{PF}}^{\text{Mn}}$, reiterating the fact that these transitions, including the one at 12 K, are indeed of dielectric origin.

The role of the rare earth on the ferroelectric ordering is studied by substituting the Dy^{3+} with rare earth Ho^{3+} ion which has smaller ionic radii and similar magnetic moment. Figure 4 shows the dielectric data plotted as a function of temperature for $x = 0.1$ sample at 0, 1, 3, and 5 T magnetic field. The figure shows that the T_{C} remains unperturbed with the magnetic field up to 3 T and it shifts towards low temperature at 5 T similar to the parent DyMnO_3 compound. The trends in slope change near these transitions strongly indicate that the applied magnetic field suppresses the ferroelectric ordering and favors a polarization flip from *c* to *a* axis. However, the $T_{\text{PF}}^{\text{Mn}}$, which was observed at 12 K in DyMnO_3 , is now vanished even without applying the field. This suggests that the spiral magnetic ordering responsible for ferroelectricity along the *a*-axis also weakens upon Ho^{3+} substitution.²⁷

To investigate the magnetoelectric coupling, the dielectric constant is measured as a function of the magnetic field at 10 K. The magnetoelectric coupling strength is measured as $\% \Delta \epsilon_r = [(\epsilon(H) - \epsilon(0))/\epsilon(0)] \times 100$, where $\epsilon(H)$ and $\epsilon(0)$ are the dielectric constant with and without field. The $\% \Delta \epsilon_r$ plotted against the field H , for the orthorhombic DyMnO_3 , is shown in Fig. 5(a). Upon varying the field H , the $\% \Delta \epsilon_r$ increases up to 3.5 T and shows the maximum value of 10. The high value of $\% \Delta \epsilon_r$ reflects the strong magnetoelectric response in the compound. With further increase in H , the $\% \Delta \epsilon_r$ starts to decrease up to 7 T and remains constant

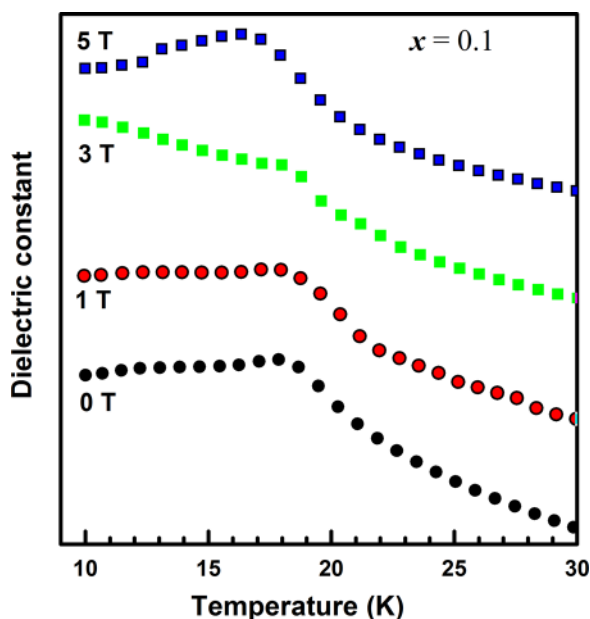


FIG. 4. Dielectric constant as a function of temperature for $\text{Dy}_{0.9}\text{Ho}_{0.1}\text{MnO}_3$ at 0, 1, 3, and 5 T magnetic field.

thereafter. Between 3.5 T and 7 T, the $\% \Delta \epsilon_r$ shows a hysteresis behavior. The switchable nature of the magnetodielectric response on reversing the magnetic field direction indicates the inherent response of the material. The increase in $\% \Delta \epsilon_r$ and its peak at 3.5 T may be attributed to the competition between the polarization along the c to a -axis and the polarization switching from c to a -axis, respectively. It is interesting to note that the magnetoelectric response observed in

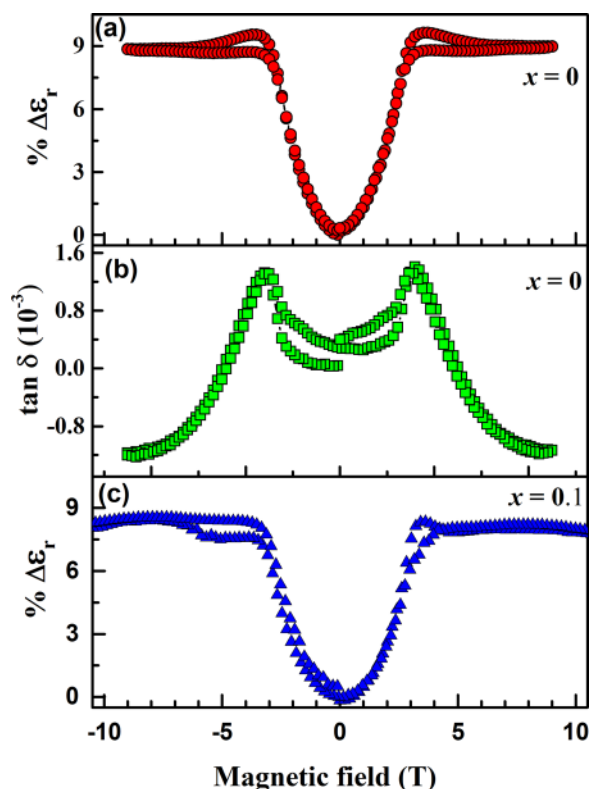


FIG. 5. The magnetic field-dependent (a) $\% \Delta \epsilon_r$ and (b) $\tan \delta$ for DyMnO_3 . (c) The magnetic field-dependent $\% \Delta \epsilon_r$ for $\text{Dy}_{0.9}\text{Ho}_{0.1}\text{MnO}_3$.

orthorhombic DyMnO_3 is two orders of magnitude larger than that of hexagonal HoMnO_3 .²⁷ The dielectric loss shown in Fig. 5(b) also concurs with the above features. The dielectric loss shows a peak at 3.5 T corresponding to the polarization switching from c to a axis, reaffirming the dielectric nature of the transition.

The $\% \Delta \epsilon_r$ plotted for $x=0.1$ samples as a function of H is shown in Fig. 5(c). The figure shows that the maximum value of $\% \Delta \epsilon_r$ is 8 which indicate the decrease in the magnetoelectric effect upon Ho^{3+} substitution. This trend is clearly seen in samples with higher values of x (not shown in figure). Upon doping with smaller ionic radii element in DyMnO_3 , the tilting of MnO_6 octahedra will increase and thereby enhance the Mn-O-Mn orbital overlap. Hence, a strong magnetoelectric coupling is expected in the Ho^{3+} doped DyMnO_3 . On the other hand, the spiral magnetic moment vector also plays an important role in determining the magnetoelectric coupling strength through Dzyaloshinskii-Moriya interaction. As inferred from Figs. 3 and 4, Ho^{3+} substitution weakens the long range spiral magnetic ordering of Mn^{3+} with the resultant suppression of the spiral magnetic moment vector. Thus in $\text{Dy}_{1-x}\text{Ho}_x\text{MnO}_3$, the breaking of the spiral magnetic ordering overwhelms the enhancement of the orbital overlap. As a result, the $\% \Delta \epsilon_r$ shows a lower value with Ho^{3+} substitution. In addition, the open loop behavior is also suppressed.

IV. CONCLUSIONS

The temperature-dependent dielectric constant and the dielectric loss of DyMnO_3 show transitions at 40, 18, and 12 K. The dispersive nature of the transition at 40 K indicates that it could be due to the polaron hopping conduction. The frequency-independent character of the transition at 18 K corroborates its origin from the spiral spin magnetic ordering induced ferroelectric transition. Interestingly, the dielectric constant, dielectric loss, and the magnetodielectric effect strongly indicate that the transition observed at 12 K could be due to the polarization flop rather than the rare earth magnetic ordering. The magnetodielectric studies reveal that the magnetoelectric coupling strength of polycrystalline orthorhombic DyMnO_3 is stronger by two orders of magnitude in comparison to hexagonal system. The Ho^{3+} substitution in DyMnO_3 resulted in reduced antiferromagnetic and ferroelectric ordering temperatures. Surprisingly, the Ho^{3+} substitution in DyMnO_3 strongly suppressed the magnetoelectric coupling strength due to the breaking of long-range spiral magnetic ordering.

ACKNOWLEDGMENTS

Partial support from the LAFICIS program and the CNRS are acknowledged.

¹W. Eerenstein, N. D. Mathur, and J. F. Schott, *Nature* **442**, 759 (2006).

²R. Ramesh and N. A. Spaldin, *Nature Mater.* **6**, 21 (2007).

³L. D. Landau and E. M. Lifshitz, *Electrodynamics of Continuous Media* (Addison-Wesley, MA, 1960).

⁴I. E. Dzyaloshinskii, *Sov. Phys. JETP* **10**, 628 (1960).

⁵T. Kimura, T. Goto, H. Shintani, K. Ishizaka, T. Arima, and Y. Tokura, *Nature* **426**, 55 (2003).

- ⁶N. Hur, S. Park, P. A. Sharma, J. S. Ahn, S. Guha, and S.-W. Cheong, *Nature* **429**, 392 (2004).
- ⁷G. Lawes, A. B. Harris, T. Kimura, N. Rogado, R. J. Cava, A. Aharony, O. Entin-Wohlman, T. Yildirim, M. Kenzelmann, C. Broholm, and A. P. Ramirez, *Phys. Rev. Lett.* **95**, 087205 (2005).
- ⁸T. Kimura, J. C. Lashley, and A. P. Ramirez, *Phys. Rev. B* **73**, 220401(R) (2006).
- ⁹W. Prellier, M. P. Singh, and P. Murugavel, *J. Phys.: Condens. Matter* **17**, R803 (2005).
- ¹⁰H. L. Yakel, W. D. Koehler, E. F. Bertaut, and F. Forrat, *Acta Crystallogr.* **16**, 957 (1963).
- ¹¹Y. Chen, H. Yuan, G. Li, G. Tian, and S. Feng, *J. Cryst. Growth* **305**, 242 (2007).
- ¹²J. H. Lee, P. Murugavel, H. R. Ryu, D. S. Lee, J. Y. Jo, J. W. Kim, H. J. Kim, K. H. Kim, Y. H. Jo, M. H. Jung, Y. H. Oh, Y. W. Kim, J. G. Yoon, J. S. Chung, and T. W. Noh, *Adv. Mater.* **18**, 3125 (2006).
- ¹³M. Nakamura, Y. Tokunaga, M. Kawasaki, and Y. Tokura, *Appl. Phys. Lett.* **98**, 082902 (2011).
- ¹⁴M. Balli, S. Jandl, P. Fournier, S. Mansouri, A. Kukhin, Yu. V. Ivanov, and A. M. Balbashov, *J. Magn. Magn. Mater.* **374**, 252 (2015).
- ¹⁵T. Kimura and Y. Tokura, *J. Phys.: Condens. Matter* **20**, 434204 (2008).
- ¹⁶T. Kimura, G. Lawes, T. Goto, Y. Tokura, and A. P. Ramirez, *Phys. Rev. B* **71**, 224425 (2005).
- ¹⁷Y. S. Chai, Y. S. Oh, L. J. Wang, N. Manivannan, S. M. Feng, Y. S. Yang, L. Q. Yan, C. Q. Jin, and K. H. Kim, *Phys. Rev. B* **85**, 184406 (2012).
- ¹⁸T. Goto, T. Kimura, G. Lawes, A. P. Ramirez, and Y. Tokura, *Phys. Rev. Lett.* **92**, 257201 (2004).
- ¹⁹R. Feyerherm, E. Dudzik, A. U. B. Wolter, S. Valencia, O. Prokhnenko, A. Maljuk, S. Landsgesell, N. Aliouane, L. Bouchernoire, S. Brown, and D. N. Argyriou, *Phys. Rev. B* **79**, 134426 (2009).
- ²⁰R. Feyerherm, E. Dudzik, N. Aliouane, and D. N. Argyriou, *Phys. Rev. B* **73**, 180401(R) (2006).
- ²¹S. Harikrishnan, S. Robler, C. M. Naveen Kumar, H. L. Bhat, U. K. Robler, S. Wirth, F. Steglich, and S. Elizabeth, *J. Phys.: Condens. Matter* **21**, 096002 (2009).
- ²²F. Schrettle, P. Lunkenheimer, J. Hemberger, V. Y. Ivanov, A. A. Mukhin, A. Balbashov, and A. Loidl, *Phys. Rev. Lett.* **102**, 207208 (2009).
- ²³M. Shao, S. Cao, S. Yuan, J. Shang, B. Kang, B. Lu, and J. Zang, *Appl. Phys. Lett.* **100**, 222404 (2012).
- ²⁴J. Strempler, B. Bohnenbuck, M. Mostovoy, N. Aliouane, D. N. Argyriou, F. Schrettle, J. Hemberger, A. Krimmel, and M. V. Zimmermann, *Phys. Rev. B* **75**, 212402 (2007).
- ²⁵I. Dzyaloshinsky, *J. Phys. Chem. Solids* **4**, 241 (1958).
- ²⁶P. J. Brown and T. Chatterji, *J. Phys.: Condens. Matter* **18**, 10085 (2006).
- ²⁷J. Magesh, P. Murugavel, R. V. K. Mangalam, K. Singh, Ch. Simon, and W. Prellier, *Appl. Phys. Lett.* **101**, 022902 (2012).
- ²⁸J. Yang, J. He, J. Y. Zhu, W. Bai, L. Sun, X. J. Meng, X. D. Tang, C. G. Duan, D. Remiens, J. H. Qiu, and J. H. Chu, *Appl. Phys. Lett.* **101**, 222904 (2012).
- ²⁹M. Mouallem-Bahout, O. Pena, D. Gutierrez, P. Duran, and C. Moure, *Solid State Commun.* **122**, 561 (2002).
- ³⁰N. Zhang, S. Dong, Q. Zang, L. Lin, Y. Y. Guo, J. M. Liu, and Z. F. Ren, *Appl. Phys. Lett.* **98**, 012510 (2011).